

SPECTRAL ANALYSIS OF YSOs AND OTHER EMISSION-LINE STARS IN THE NORTH AMERICA AND PELICAN NEBULAE REGION

C. J. Corbally¹, V. Straižys² and V. Laugalys²

¹ *Vatican Observatory Research Group, Steward Observatory, Tucson, Arizona 85721, U.S.A.; corbally@as.arizona.edu*

² *Institute of Theoretical Physics and Astronomy, Vilnius University, Goštauto 12, Vilnius LT-01108, Lithuania; straižys@itpa.lt*

Received 2009 June 20; accepted 2009 September 15

Abstract. Far red spectra for 34 stars with V magnitudes between 15 and 18 in the direction of the North America and Pelican nebulae (NAP) star-forming region are obtained. Some of these stars were known earlier as emission-line objects, others were suspected as pre-main-sequence stars from photometry in the J , H , K_s and *Vilnius* systems. We confirm the presence of the $H\alpha$ line emission in the spectra of 19 stars, some of them exhibit also emission in the OI and CaII lines. In some of the stars the $H\alpha$ absorption line is filled with emission. To estimate their evolutionary status, the spectral energy distributions, based on *Vilnius*, 2MASS, MSX and *Spitzer* photometry, are applied. Only eight emission-line stars are found to be located at a distance of the NAP complex. Others are either chromospherically active stars in front of the complex or distant luminous stars with $H\alpha$ absorption and emission components. For five stars with faint emission the data are not sufficient to estimate their distance. One star is found to be a heavily reddened K-supergiant located in the Outer arm. The stars, for which we failed to confirm the emission in $H\alpha$, are mostly red dwarfs located in front of the NAP complex, two of them could be binaries with L-type components. Taking into account the stars suspected to be YSOs by their 2MASS colors we conclude that the NAP complex can possess a considerable population of young stars hidden behind the dust cloud.

Key words: stars: pre-main sequence – stars: emission-line – star-forming regions: individual (North America, Pelican)

1. INTRODUCTION

The complex of two emission nebulae, known as North America and Pelican (hereafter NAP), and the dust/molecular clouds between them, is one of the nearest star-forming regions located at a distance of ~ 500 pc. Since Herbig's (1958) discovery it has been known to contain a number of T Tauri and other $H\alpha$ emission stars. The largest number of young stars is found in the Pelican Nebula (IC 5070), a few in the North America near Florida and in the Gulf of Mexico. Although later investigations in the area have revealed more emission-line stars or young objects

Table 1. List of the investigated stars in which emission lines or emission components were found. For the Laugalys et al. (2006) stars, V is the green *Vilnius* magnitude rounded to the nearest 0.1 mag, and F is the red photographic magnitude taken from GSC 2.3.2 (Lasker et al. 2008). In the last column, spectral types are from Laugalys et al. (2006), and YSO means a suspected young stellar object selected from the infrared sources (see the text). For them both V and F magnitudes are from GSC 2.3.2.

Name	RA (2000)	DEC (2000)	ℓ	b	V	F	Type
II-64	20:57:07.57	+43:41:59.7	84.829	-1.170	17.6	15.3	k-m V,T?
II-77	20:57:22.25	+43:57:53.4	85.059	-1.031	15.1	13.6	k0 V,e?
II-108*	20:57:48.80	+43:50:23.6	85.016	-1.173	16.6	14.5	k-m V,T?
II-109	20:57:50.06	+43:50:57.0	85.026	-1.170	17.9	16.0	m1 V,e?
II-113*	20:57:56.51	+43:52:36.3	85.059	-1.166	16.3	14.4	k6 V,e?
II-114	20:57:57.50	+43:50:09.0	85.030	-1.195	17.0	14.9	m2 V,e?
II-117*	20:57:59.87	+43:53:26.0	85.076	-1.165	15.5	13.3	T?
II-122	20:58:06.05	+43:49:33.0	85.039	-1.221	17.7	15.0	k-m V,e?
III-85	20:59:35.36	+43:52:03.7	85.247	-1.397	16.6	15.1	g,e?
IV-5	20:53:51.88	+44:24:10.1	84.986	-0.268	16.7	15.0	T?
IV-39	20:54:25.54	+44:23:02.0	85.036	-0.357	17.4	15.4	k-m, e?
IV-62	20:54:45.36	+44:33:02.8	85.202	-0.295	17.2	13.4	k0 V,e?
IV-98	20:55:11.23	+44:24:05.3	85.138	-0.450	16.2	14.2	Be:
CSL 3	20:48:50.70	+43:49:49.6	83.971	+0.062		16.6	YSO
CSL 4	20:49:32.19	+44:17:03.1	84.402	+0.252		16.2	YSO
CSL 5	20:53:38.46	+44:28:48.4	85.020	-0.188		17.0	YSO
CSL 6	20:54:46.90	+44:48:19.7	85.400	-0.134	17.6	15.3	YSO
CSL 7	20:56:27.82	+45:25:23.4	86.062	+0.039	18.4	16.3	YSO
CSL 8	21:01:04.87	+43:42:34.0	85.305	-1.704		15.3	YSO

Note. The three stars with the asterisked numbers are observed and classified independently by Laugalys et al. (2006) in two overlapping areas, Area II and Area III, located in the Gulf of Mexico. Their numbers in Table 2 and Table 3 of the 2006 paper are: II-108 = III-1, II-113 = III-4 and II-117 = III-6.

(Welin 1973; Giesekeing 1973; Tsvetkov 1975; Giesekeing & Schumann 1976; Marcy 1980; Kohoutek & Wehmeyer 1997; Witham et al. 2008), the NAP complex is considered a star-forming region (SFR) not as active as the Taurus-Auriga complex or the Orion association. Most of the discovered young objects are located at the edges of the dust clouds. The discovery by Laugalys et al. (2006) of a group of K and M dwarfs in the direction of the dark cloud LDN 935, having signs of $H\alpha$ emission, was an indication that a hidden population of young stars could exist within or behind the dust clouds.

In the latter investigation, about 40 stars, mostly K and M dwarfs, were suspected to be pre-main-sequence (hereafter PMS) objects on the basis of photometric classification using seven-color CCD photometry in the *Vilnius* system down to $V = 17$ – 18 mag. The presence of $H\alpha$ emission was detected as an excessive radiation in the S filter at 656 nm, i.e., placed on the $H\alpha$ line. For this, the interstellar reddening-free diagrams Q_{XZS} vs. Q_{XYV} and Q_{XZS} vs. Q_{YZV} were used (Straižys et al. 1998). Many of the suspected emission-line stars also exhibited infrared excesses, four of them were known PMS stars. It was supposed that the detected stars belong to either the classical T Tauri or post-T Tauri groups and are affected by considerable interstellar reddening.

An additional group of suspected young stellar objects (YSOs) with infrared

excesses in the NAP area has been selected using near- and medium- infrared photometry taken from the 2MASS and MSX surveys (see Section 2). The IRAS survey data in most of the NAP complex are not available, except for the part of the area with the smallest right ascensions. For 34 brightest stars from both groups of the suspects we made spectral observations to confirm or disprove their possible PMS status. In Section 3 we describe our spectral observations and their results. The search for mid-infrared excesses in the spectral energy distributions is described in Section 4 and the search for X-ray sources in Section 5. Discussion of the results for individual stars is given in Section 6. The last section gives a summary of the results.

2. YSOs SUSPECTED FROM INFRARED SURVEYS

The list of suspected YSOs was obtained in the way similar to that applied in the Camelopardalis dark clouds (Straizys & Laugalys 2007).

1. From the 2MASS catalog we selected 98 924 stars in a $3^\circ \times 3^\circ$ area with the center close to the Comerón & Pasquali (2005) O-type star (J2000.0: 20:56 = 314.0°, +44.0°) and having errors of the J , H and K_s magnitudes ≤ 0.05 mag.

2. From this sample, 80 stars, satisfying the condition $Q_{JHK_s} \leq 0.0$, were selected. Here,

$$Q_{JHK_s} = (J - H) - (E_{J-H}/E_{H-K_s})(H - K_s), \quad (1)$$

with the ratio of color excesses $E_{J-H}/E_{H-K_s} = 2.0$ taken from Straizys et al. (2008).

Apart from YSOs, this list contains also heavily reddened O–B stars, oxygen-rich AGB stars (SR variables, Miras and OH/IR objects), carbon-rich AGB stars of spectral type N and cool red dwarfs of spectral types M5–M10 and L. The problem of recognizing stars of these types was discussed in our earlier paper devoted to search for O-type stars behind the LDN 935 cloud (Straizys & Laugalys 2008). Miras, carbon stars and non-stellar sources were excluded on account of information from the Simbad database. Unfortunately, many objects in the list of YSO suspects are absent in the Simbad identifier of astronomical objects. However, their near red and far red magnitudes are available in the IPHAS survey (Drew et al. 2005; González-Solares et al. 2008). Magnitudes or fluxes of some of the objects have been also found in the MSX (Egan et al. 2003) and the photographic GSC 2.3.2 catalog (Lasker et al. 2008) at Simbad.

From the list of YSOs, suspected by their 2MASS colors, we took only eight brightest objects down to magnitude $r = 17$. These stars are denoted by initials of the authors (CSL) and the number (from 1 to 8). The fainter objects were not practical for spectral observations with the Steward 2.3 m telescope.

3. FAR-RED SPECTRAL OBSERVATIONS

For spectral observations we selected 34 stars. Among these, emission in H α was found in 19, including six spectra where the absorption line is filled by emission, and in 16 stars no sign of emission was seen. Table 1 gives the list of stars with H α emission; they are identified in Figure 1. The objects for which emission lines were absent are listed in Table 3.

Spectra for most stars were taken on 2007 October 21–23 with the Boller & Chivens spectrograph on the Steward Observatory 2.3 m telescope at Kitt

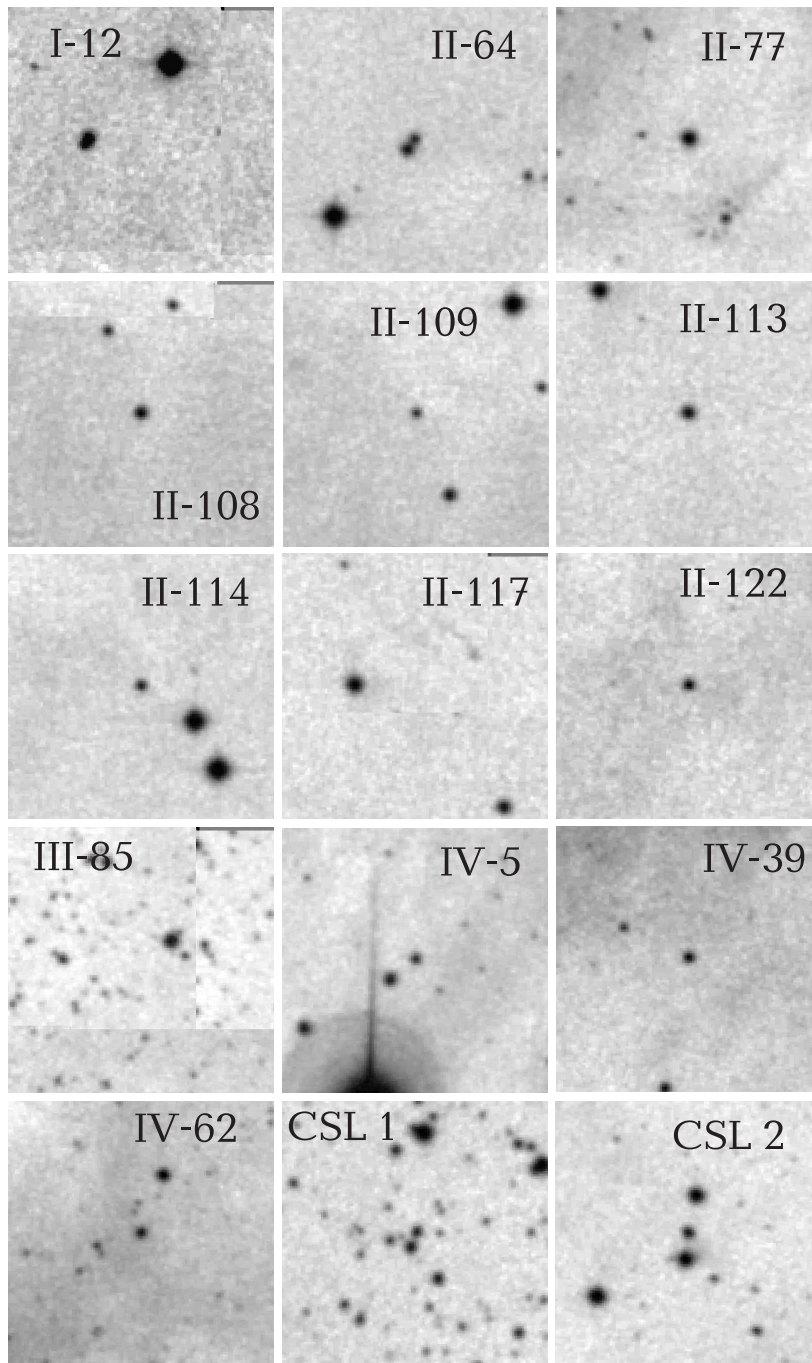


Fig. 1. Identification charts. The fields of $1.8' \times 1.8'$ sizes are DSS2 red copies taken from the Internet's Virtual Telescope SkyView. The identified star is always in the center.

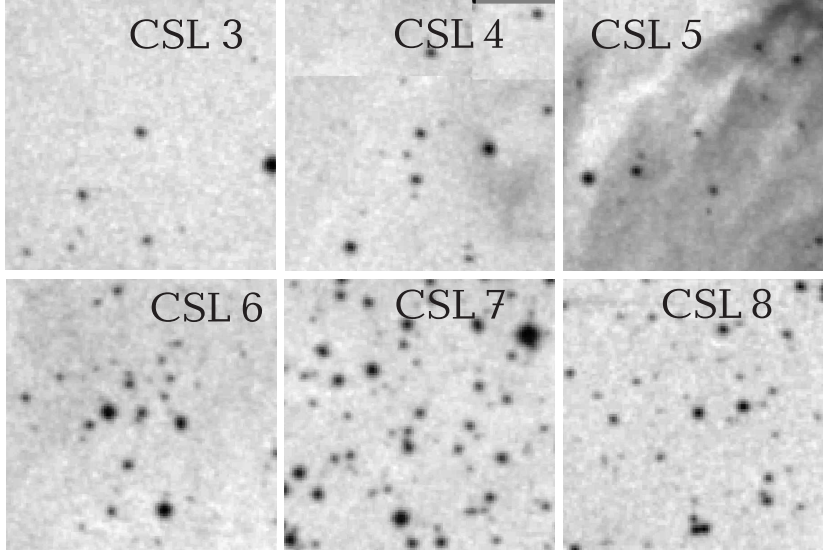


Fig. 1. Continued.

Peak, with a resolution of 5.7 \AA and a range from 607 to 939 nm on the BCSpec 1200×800 CCD detector. The slit width was $1.5''$. Spectra of the CSL stars and of IV-62, IV-88 and IV-98 were taken on 2008 October 19–21 with the same spectrograph and detector setup. Reductions of the spectra are described in our previous papers which present the results for suspected YSOs in the Camelopardalis clouds (Corbally & Straizys 2008, 2009).

The spectra with emission signs in $H\alpha$ are shown in a widened form in Figure 2 and their energy distributions in Figures 3 (a–r). The equivalent widths of the prominent emission features ($H\alpha$, CaII triplet, OI at 8498 \AA and P9 at 9226 \AA), measured with the IRAF ‘splot’ utility, are given in Table 2. The emission in the $H\alpha$ line in some stars does not appear above the continuum but fills the absorption line or looks like an emission component within the absorption line. The last column of Table 2 gives the spectral type obtained using the criteria described by Danks & Dennefeld (1994).

4. SPECTRAL ENERGY DISTRIBUTIONS IN THE INFRARED

The most important confirmation that a star belongs to PMS stars (or YSOs) is the presence of continuous emission in the infrared range with $\lambda > 3 \mu\text{m}$, which originates from dust envelopes or disks. Therefore we constructed for the investigated stars the spectral energy distributions (SEDs) in the form $\log \lambda F_\lambda$ vs. λ from 0.55 to $24 \mu\text{m}$, taking their photometry results in different systems. Here λ is in μm and F_λ in $\text{erg} \times \text{cm}^{-2} \times \text{s}^{-1} \times \mu\text{m}^{-1}$. The V magnitudes were taken from *Vilnius* photometry (Laugalys et al. 2006) or from GSC 2.3.2. The r and i magnitudes are from IPHAS, the infrared magnitudes are from 2MASS, MSX and *Spitzer* surveys. The *Spitzer* I_1 , I_2 , I_3 , I_4 and M_1 data were taken from Guieu et al. (2009) or were kindly communicated by L. M. Rebull.

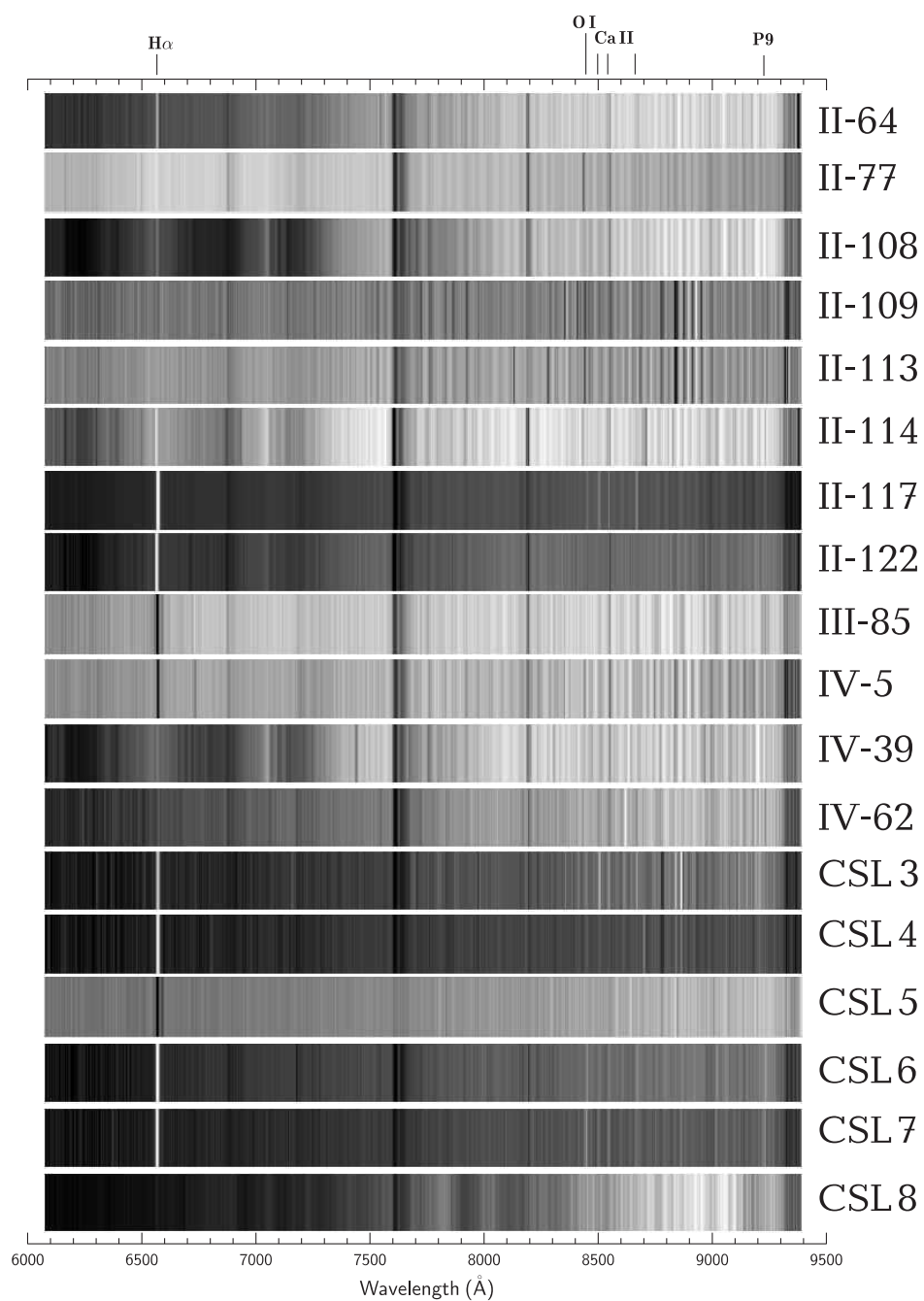


Fig. 2. The widened spectra of stars with the emission in $H\alpha$. The telluric H_2O and O_2 bands are not excluded.

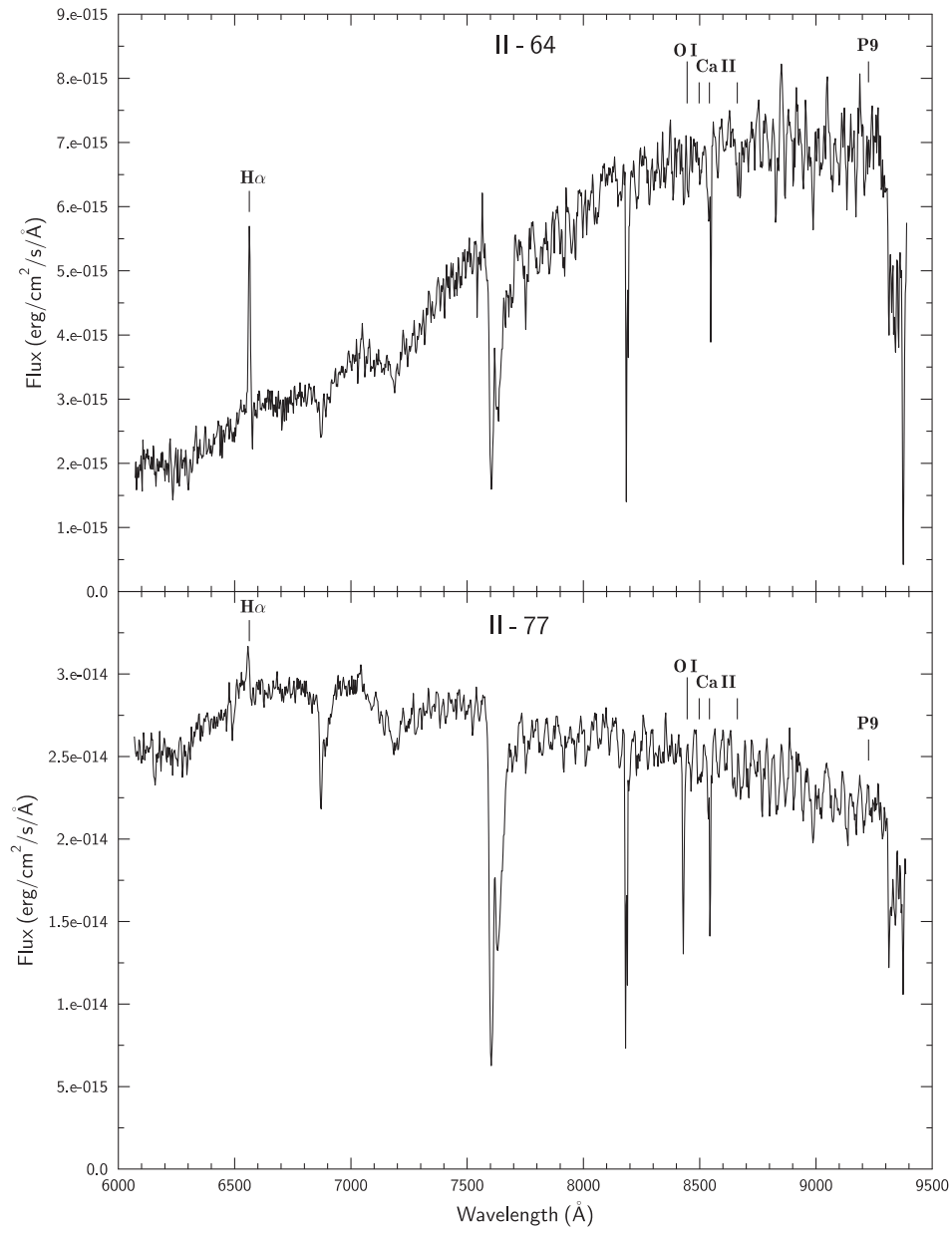


Fig. 3a and 3b. Spectra of the stars II-64 and II-77.

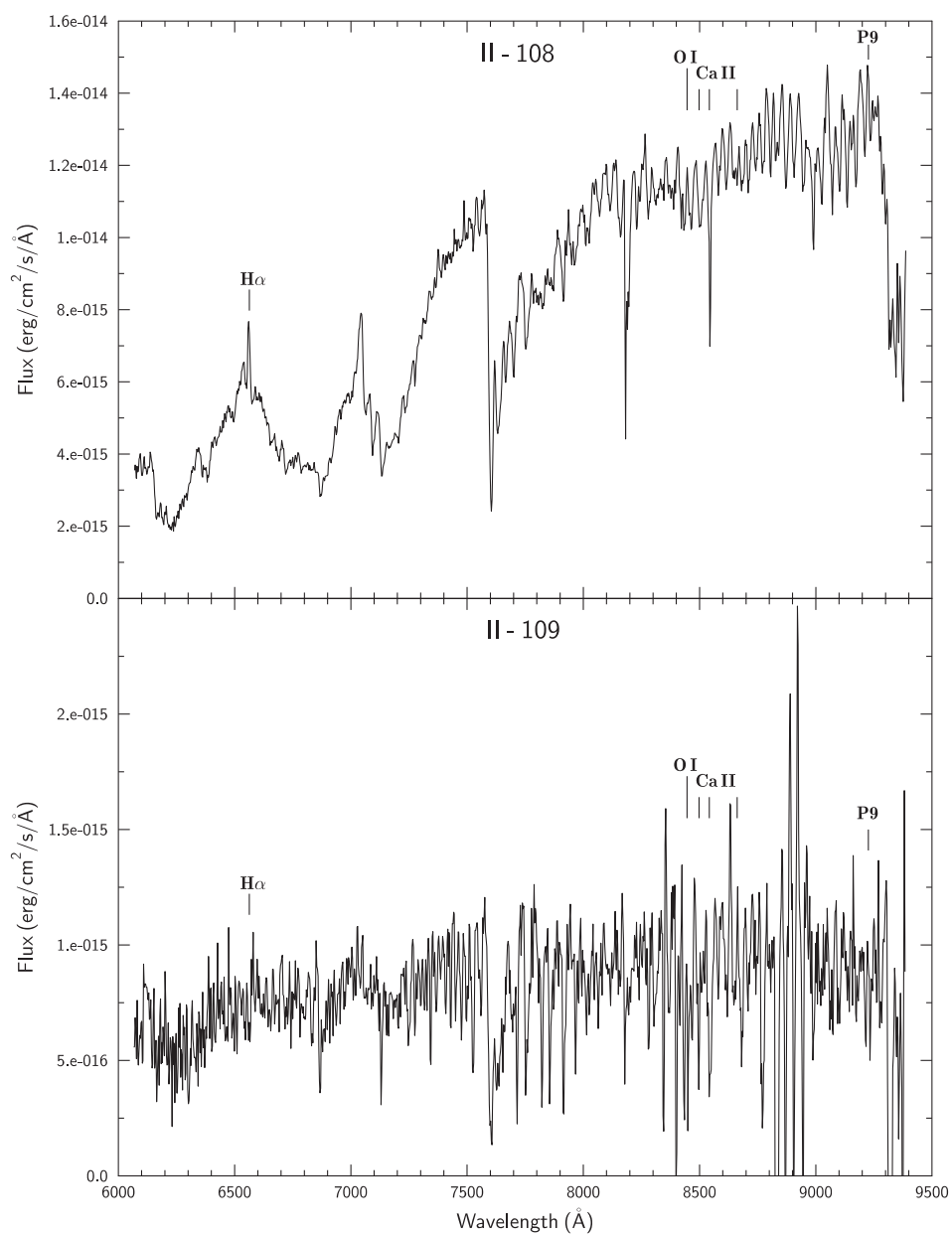


Fig. 3c and 3d. Spectra of the stars II-108 and II-109.

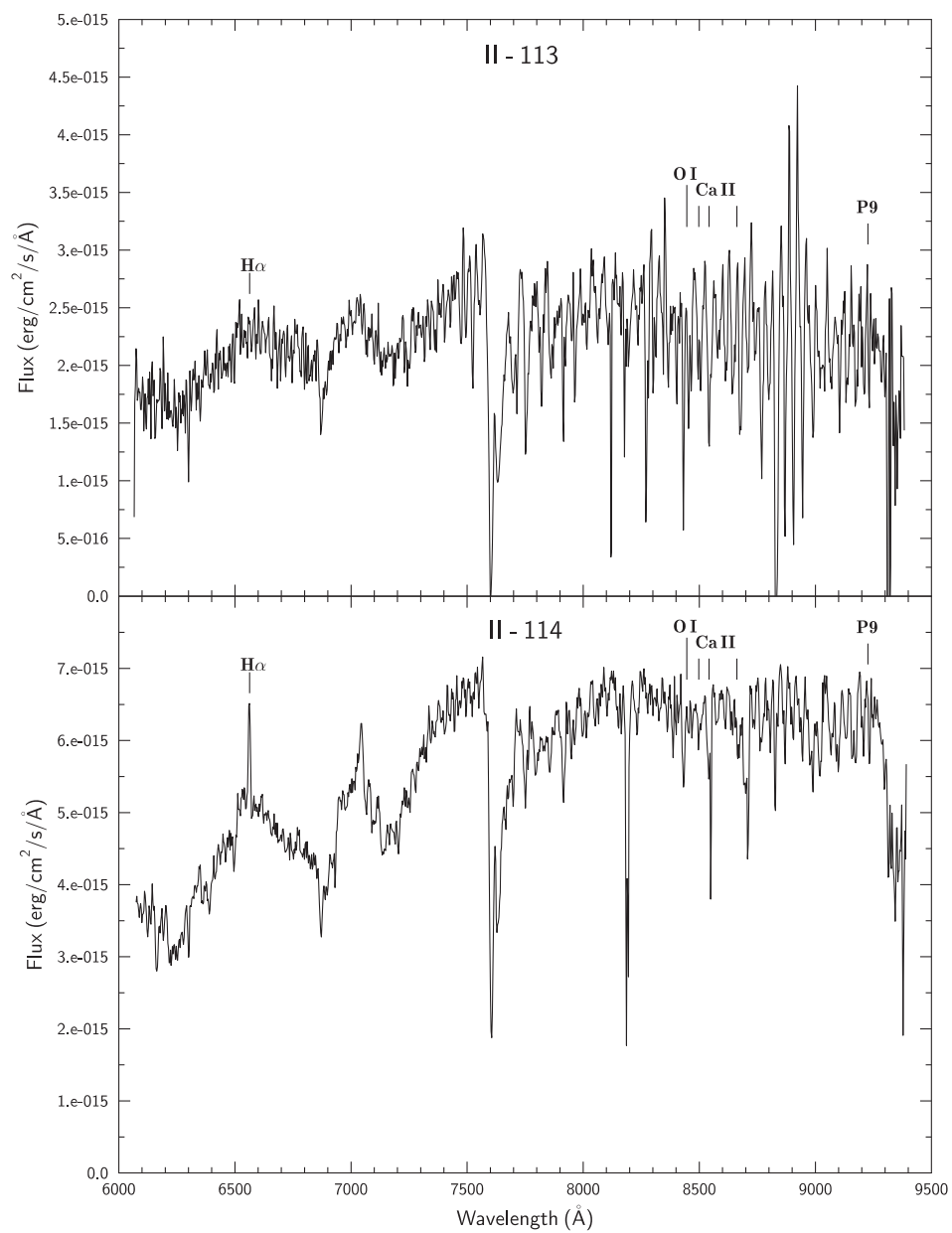


Fig. 3e and 3f. Spectra of the stars II-113 and II-114.

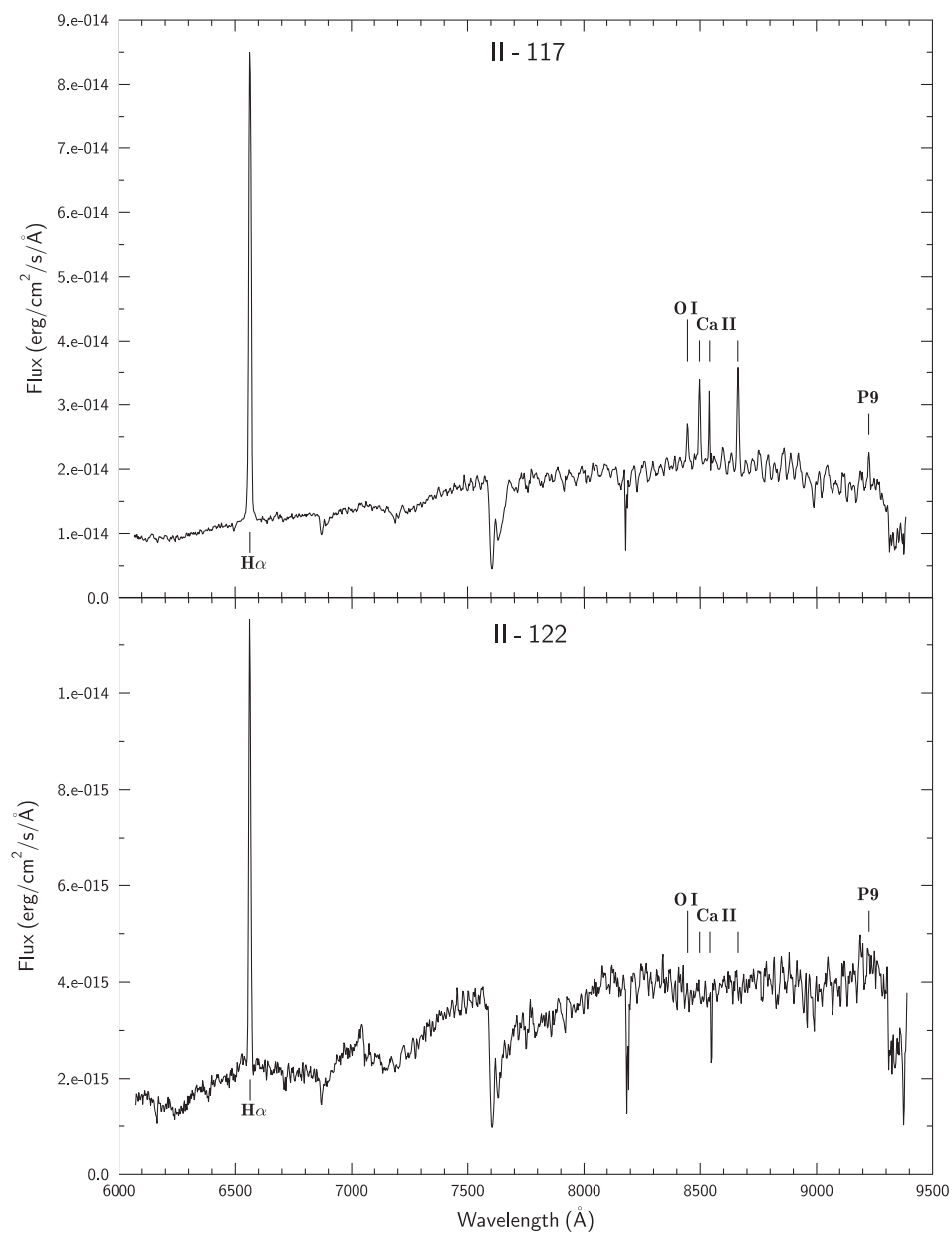


Fig. 3g and 3h. Spectra of the stars II-117 and II-122.

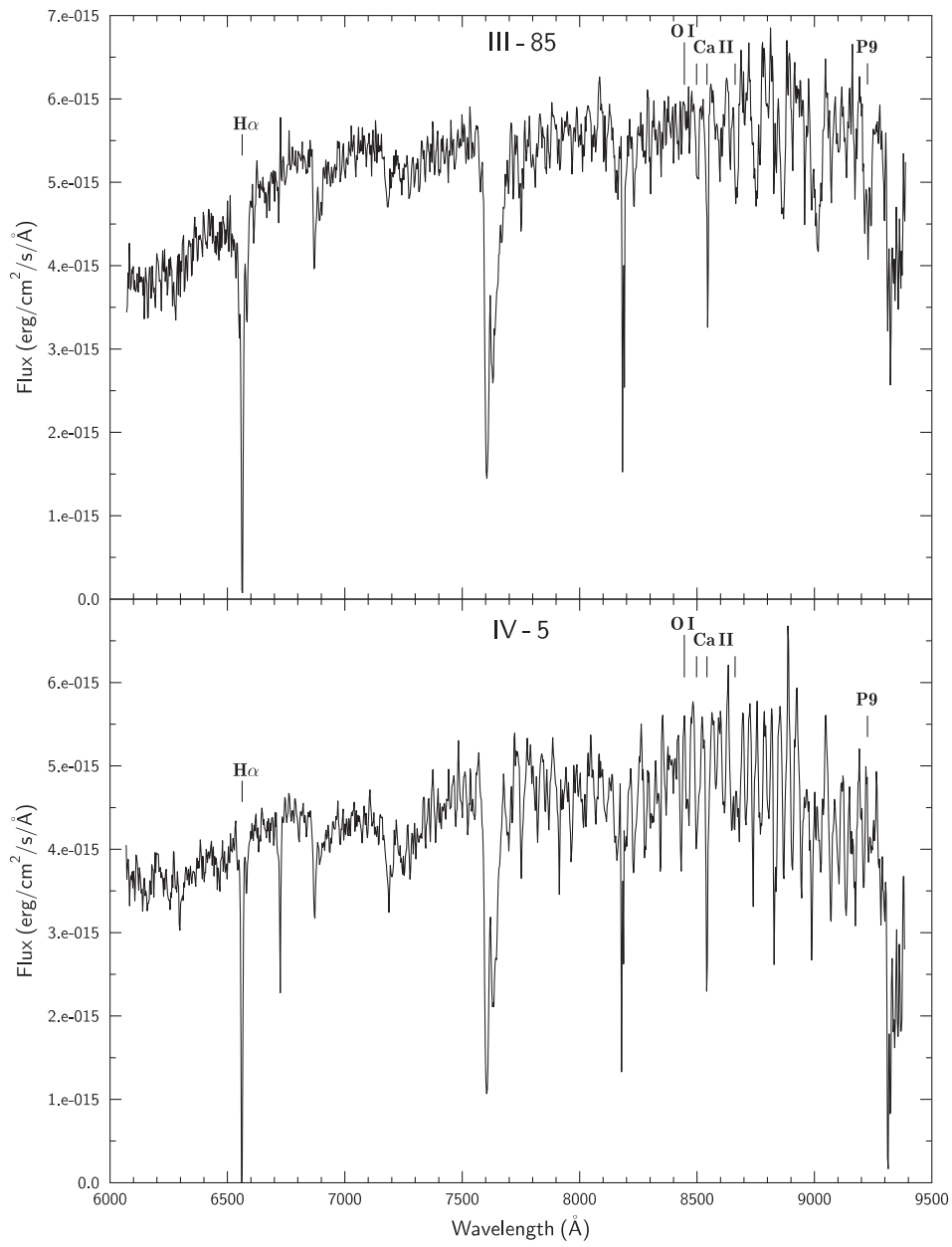


Fig. 3i and 3j. Spectra of the stars III-85 and IV-5.

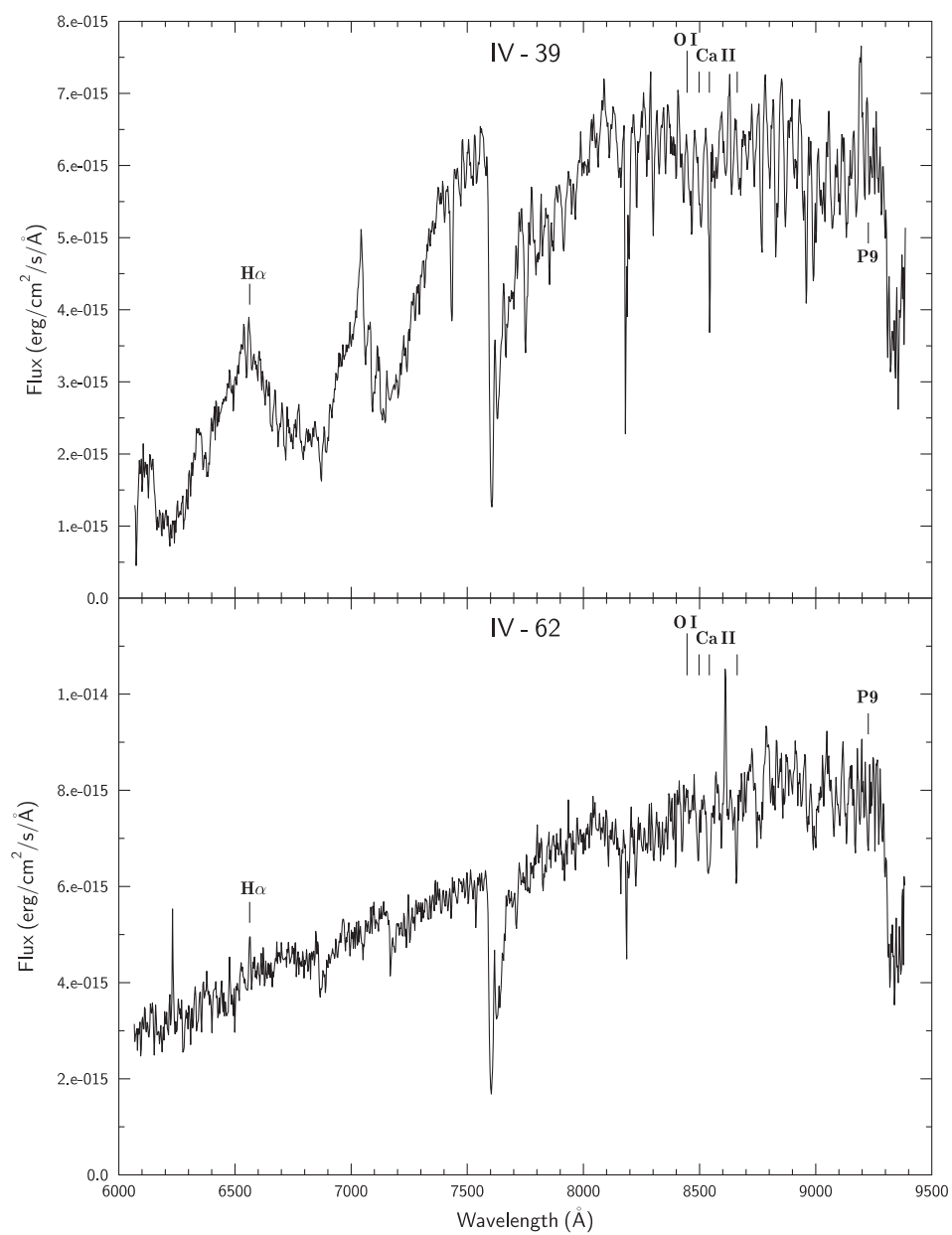


Fig. 3k and 3l. Spectra of the stars IV-39 and IV-62.

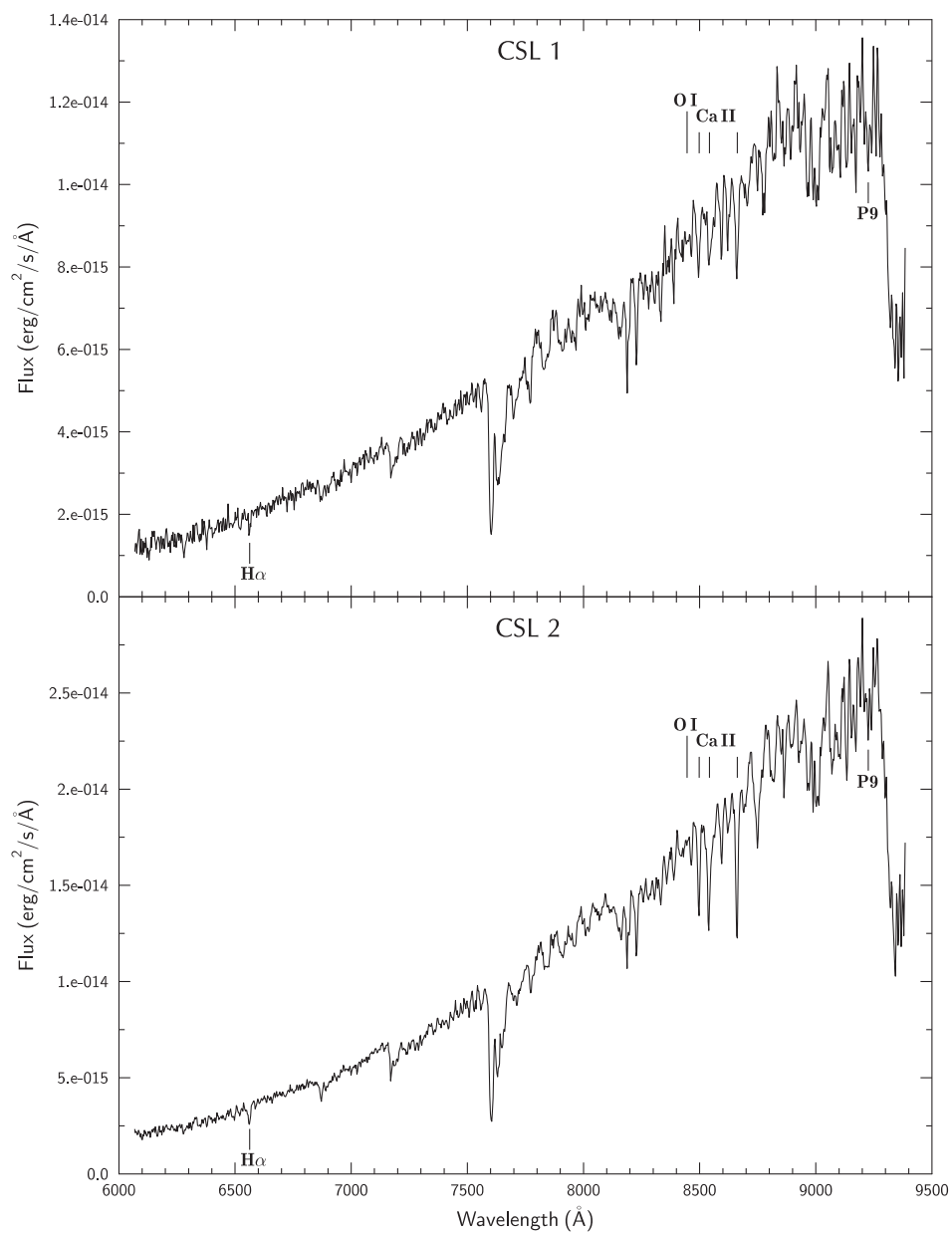


Fig. 3m and 3n. Spectra of the stars CSL 1 and CSL 2.

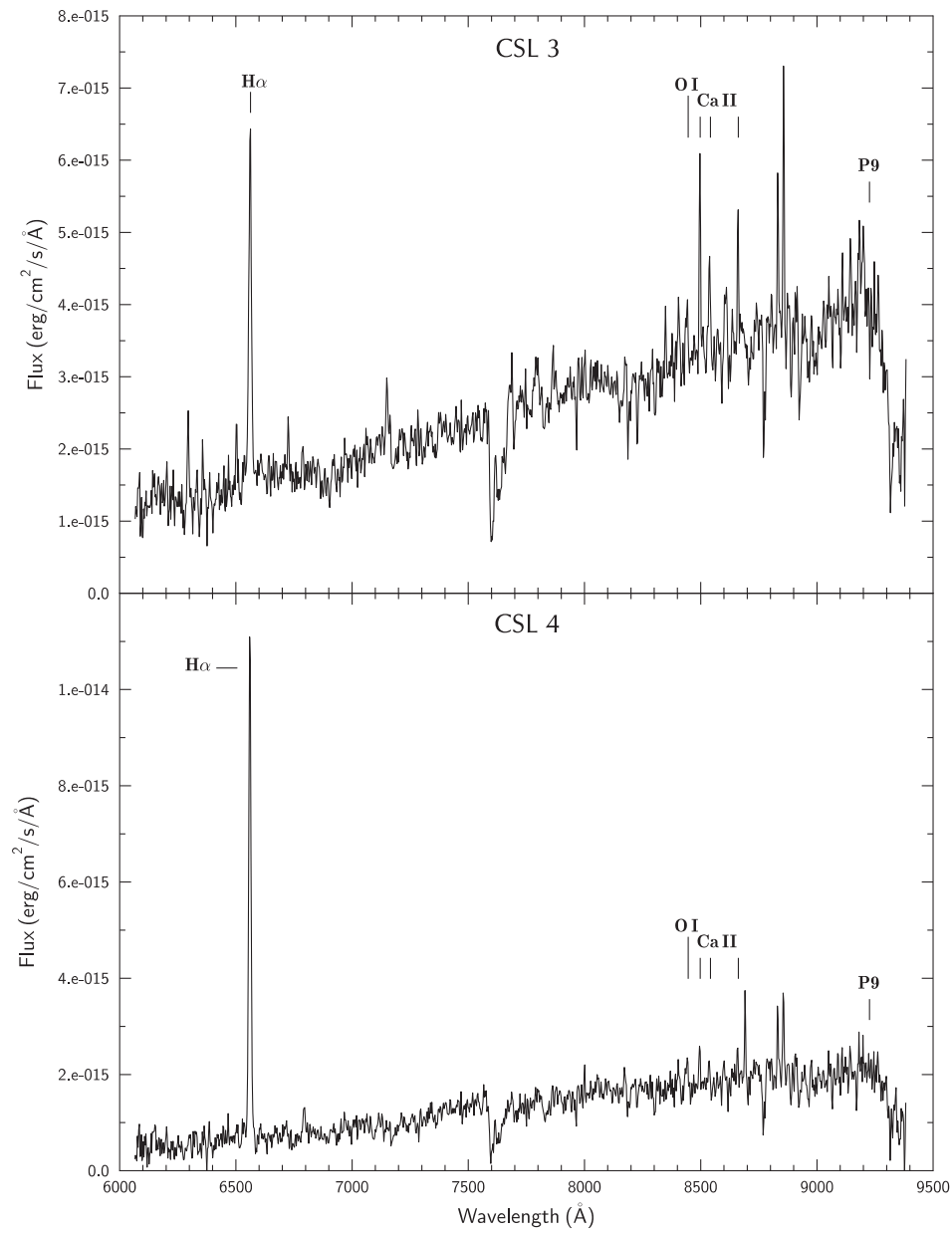


Fig. 3o and 3p. Spectra of the stars CSL 3 and CSL 4.

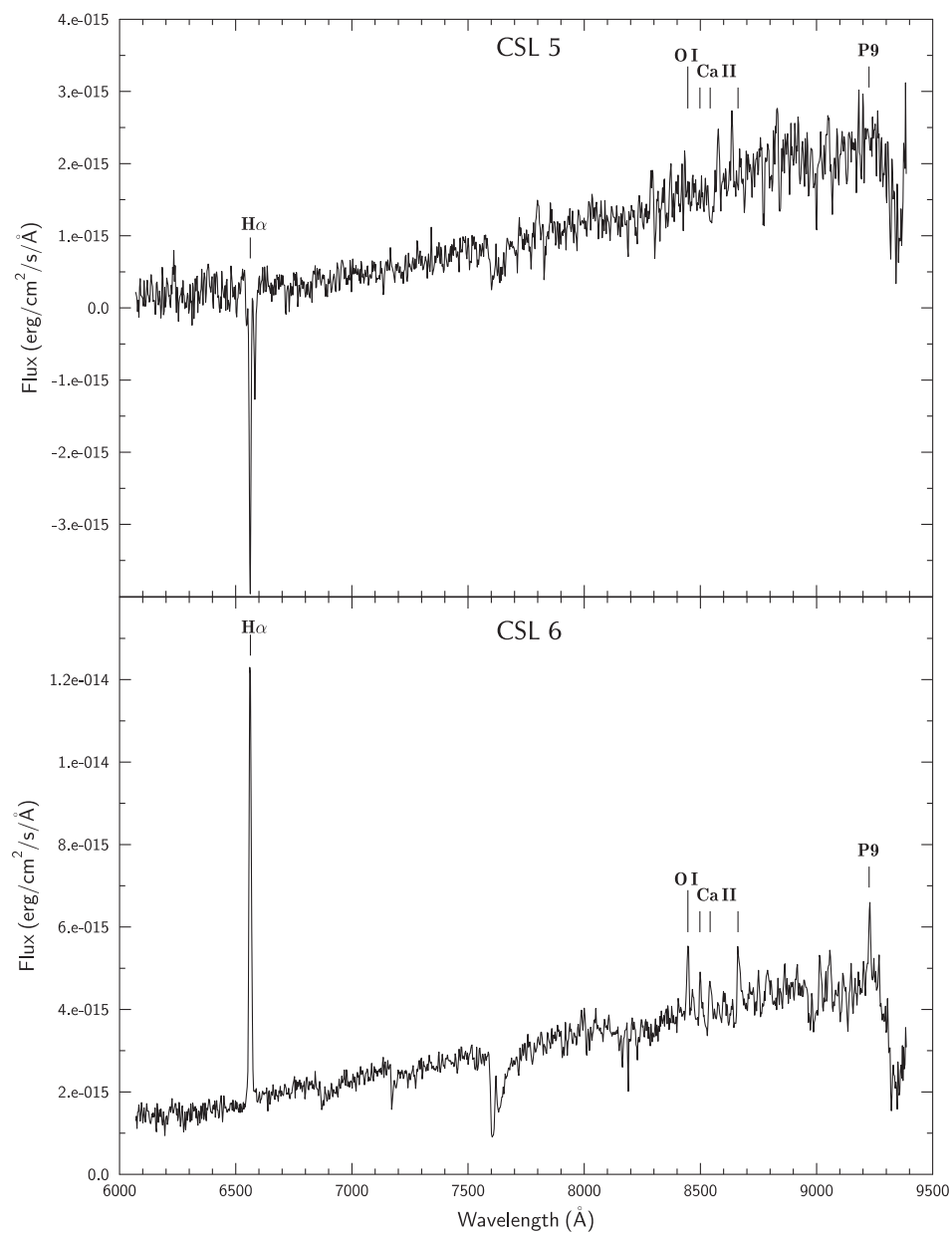


Fig. 3q and 3r. Spectra of the stars CSL 5 and CSL 6.

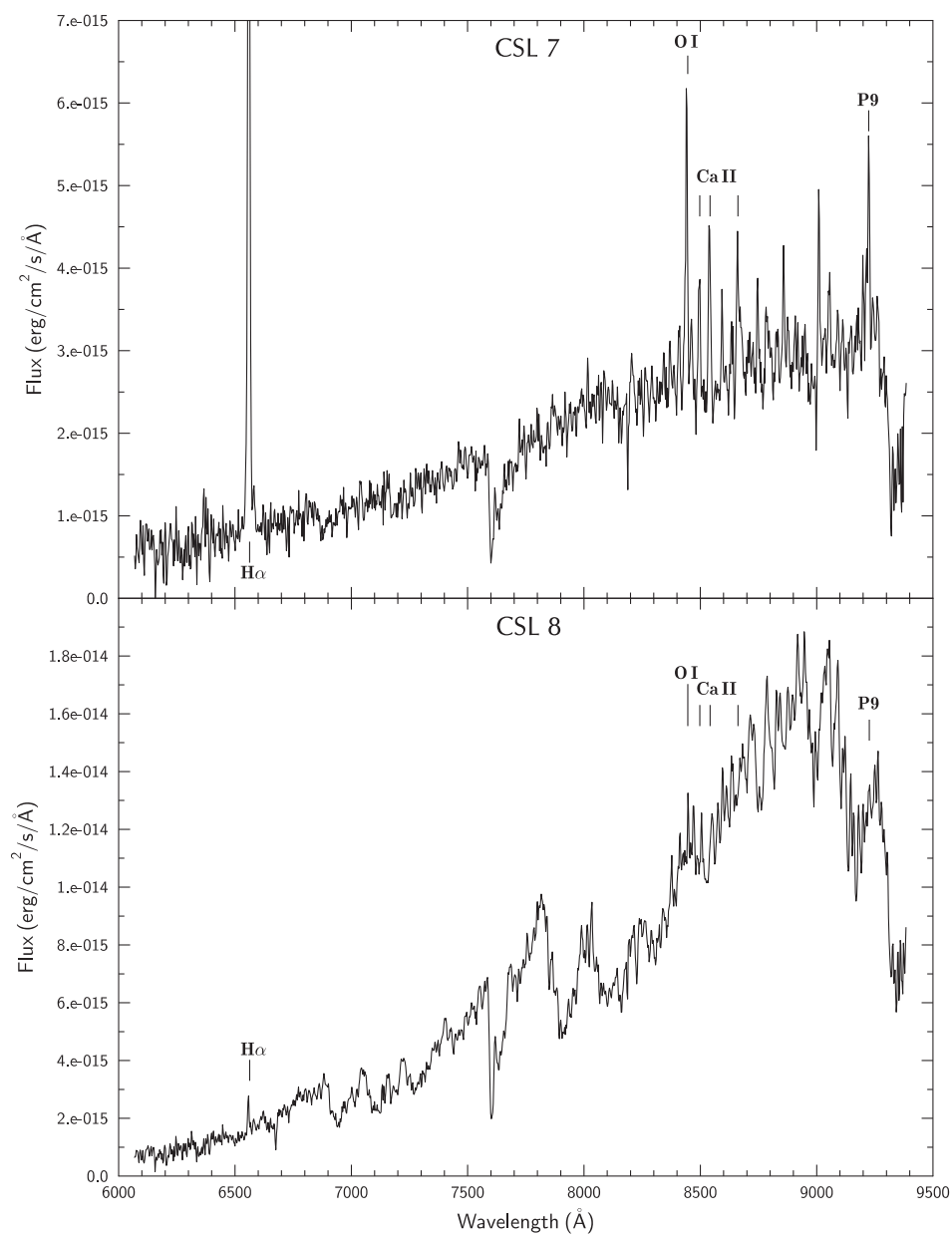


Fig. 3s and 3t. Spectra of the stars CSL 7 and CSL 8.

Table 2. Equivalent widths of emission lines and spectral classification.

Star	Obs. date	EW_{6563} H α	EW_{8446} O I	EW_{8498} Ca II	EW_{8542} Ca II	EW_{8662} Ca II	EW_{9226} P9	Spectral class
II-64	2007-10-21	-6.8						K2e (0.5)
II-77	2007-10-22	-0.7						G8e (0.1)
II-108	2007-10-21	-0.3						M3.5e (0.1)
II-109	2007-10-22							Ge
II-113	2007-10-22							Ge
II-114	2007-10-23	-1.8						M1e (0.2)
II-117	2007-10-21	-79.4	-1.8	-4.0	-1.4	-5.1	-1.2	G5 e (2)
II-122	2007-10-23	-41.1						K7e (1.5)
III-85	2007-10-23							A0e
IV-5	2007-10-21							A0e
IV-39	2007-10-21	-1.2						M3e
IV-62	2008-10-21	-1.8						K0e
IV-98	2008-10-21							B5(e)
CSL 3	2008-10-19	-30.5		-4.1	-1.9	-2.4		G0e (2)
CSL 4	2008-10-19	-151.3		-2.9	-1.7	-5.4		F0e (4)
CSL 5	2008-10-21							A5(e)
CSL 6	2008-10-20	-82.9	-3.2			-3.9		A0e (3)
CSL 7	2008-10-20	-168.7	-11.3	-3.1	-5.8		-4.2	A0e (4)
CSL 8	2008-10-20	-5.0						K3 Ie (3)

Notes. Almost in all spectra nebular emission is seen, it is subtracted during the reductions; in stars II-109 and II-113 H α is filled in; in stars III-85, IV-5, IV-98 and CSL 5 the emission is seen in H α core.

The method of obtaining the SEDs from the GSC photometric data is described by Straižys & Laugalys (2007). For the V passband we used $\lambda = 0.55 \mu\text{m}$ and $F_{\lambda}^{m=0} = 3.66 \times 10^{-5}$.

The IPHAS r' and i' magnitudes (hereafter we will denote them simply r and i) are measured with the filters similar to the corresponding Sloan Digital Sky Survey (SDSS) filters with central wavelengths 624 nm and 774 nm. However, the IPHAS magnitudes are given in the Vega-based zero-magnitude scale while the SDSS magnitudes use the so-called AB magnitude scale related to the energy flux units Janskys:

$$F_{\nu} \text{ (Jy)} = 3631 \text{ dex}(-0.4 \text{ AB}) . \quad (2)$$

Therefore, we transformed the IPHAS magnitudes to the AB scale:

$$r \text{ (AB)} = r \text{ (IPHAS)} + 0.163, \quad (3)$$

$$i \text{ (AB)} = i \text{ (IPHAS)} + 0.387. \quad (4)$$

After that the magnitudes in the AB scale were transformed to $\log \lambda F_{\lambda}$ by the equation:

$$\log \lambda F_{\lambda} = \log[1.09 \times 10^{-5} \lambda^{-1} \times \text{dex}(-0.4 \text{ AB})]. \quad (5)$$

For the *Spitzer* passbands the following equation was used:

$$\log \lambda F_{\lambda} = \log(3 \times 10^{-9} \times \lambda^{-1} \times F_{\nu}), \quad (6)$$

with λ in μm and F_ν in Jy. The fluxes in Jy were obtained from the *Spitzer* magnitudes by the equation:

$$m = -2.5 \log(F_\nu/F_\nu^{m=0}), \quad (7)$$

where $F_\nu^{m=0}$ is the flux of Vega in the passband in Janskys. The following fluxes of Vega in the passbands I_1 , I_2 , I_3 , I_4 and M_1 were used: 280.9, 179.7, 115.0, 64.1 and 7.15 Jy.

The spectral energy distributions for 16 stars, for which fluxes in the MSX and/or *Spitzer* systems were available, are shown in Figure 4. The SEDs for the emission-line stars V521 Cyg, LkH α 189 and LkH α 191 are shown for comparison.

5. THE SEARCH FOR X-RAY SOURCES

Both classical T Tauri stars (CTTS) and post-T Tauri stars with weak emission lines (WTTS) are emitters of strong X-rays from their active coronae. Consequently, the presence of X-ray radiation is one of the main criteria for the identification of PMS objects. Therefore we decided to verify if our stars are associated with any X-ray sources.

According to an X-ray catalog search of the Goddard Space Flight Center (<http://heasarc.gsfc.nasa.gov>), X-ray sources in the region of the NAP nebulae are investigated only by the ROSAT satellite. ROSAT has observed all the sky in the 0.1–2.4 keV energy range in a scanning mode, about 14% of the sky in a pointed mode and about 1.8% of the sky in a pointed high-resolution mode. The accuracy of the coordinates is about $1'$ in the scanning mode, about $10''$ in the pointed mode and 1 – $5''$ in the pointed high-resolution mode. The limiting count rates are 0.01–0.05 ct/s in the scanning mode, 0.001–0.002 ct/s in the pointed and pointed high-resolution modes with exposures of 1–4 hours.

ROSAT scanning observations cover the whole NAP area but pointed observations are missing in the SE corner with RA $>20:58$ and DEC $<+44^\circ$. High resolution observations are available only in a circle with a radius of $20'$ at RA = 20:52, DEC = $+44:20$ and they cover the Pelican Nebula.

The following ROSAT catalogs available at CDS were searched: the bright source catalog (BSC, Voges et al. 1999), the faint source catalog (FSC, Voges et al. 2000), the catalog of HRI pointed observations (1RXH, ROSAT Team 2000a) and the 2nd catalog of pointed observations (2RXP, ROSAT Team 2000b). It was strange enough to realize that none of our objects from Table 1 could be found in these catalogs. But what is more, in the ROSAT catalogs we could not identify any known NAP T Tauri star either. In the above mentioned area in the Pelican Nebula, covered by the ROSAT high-resolution pointing observations, a number of T Tauri and H α emission line stars are known. None of them were found in the 1RXH catalog, despite the fact that the limiting photon flux in the area was about 0.01 ct/s with about 1.3 hour exposure.

Trying to find the explanation, we have checked X-ray counts given by PMS objects in the Orion association which is roughly at the same distance from the Sun as the NAP complex. In Orion, Gagne et al. (1995) were able to measure with the HRI instrument PMS objects of spectral types K and M with count rates between 0.001 and 0.03 ct/s and exposures from 3 to 8 hours. The limiting count rate 0.001 ct/s with an 8 hour exposure is equivalent to about 0.006 ct/s with an 1.3 hour exposure used in Pelican. The brightest sources in Orion (0.03 ct/s)

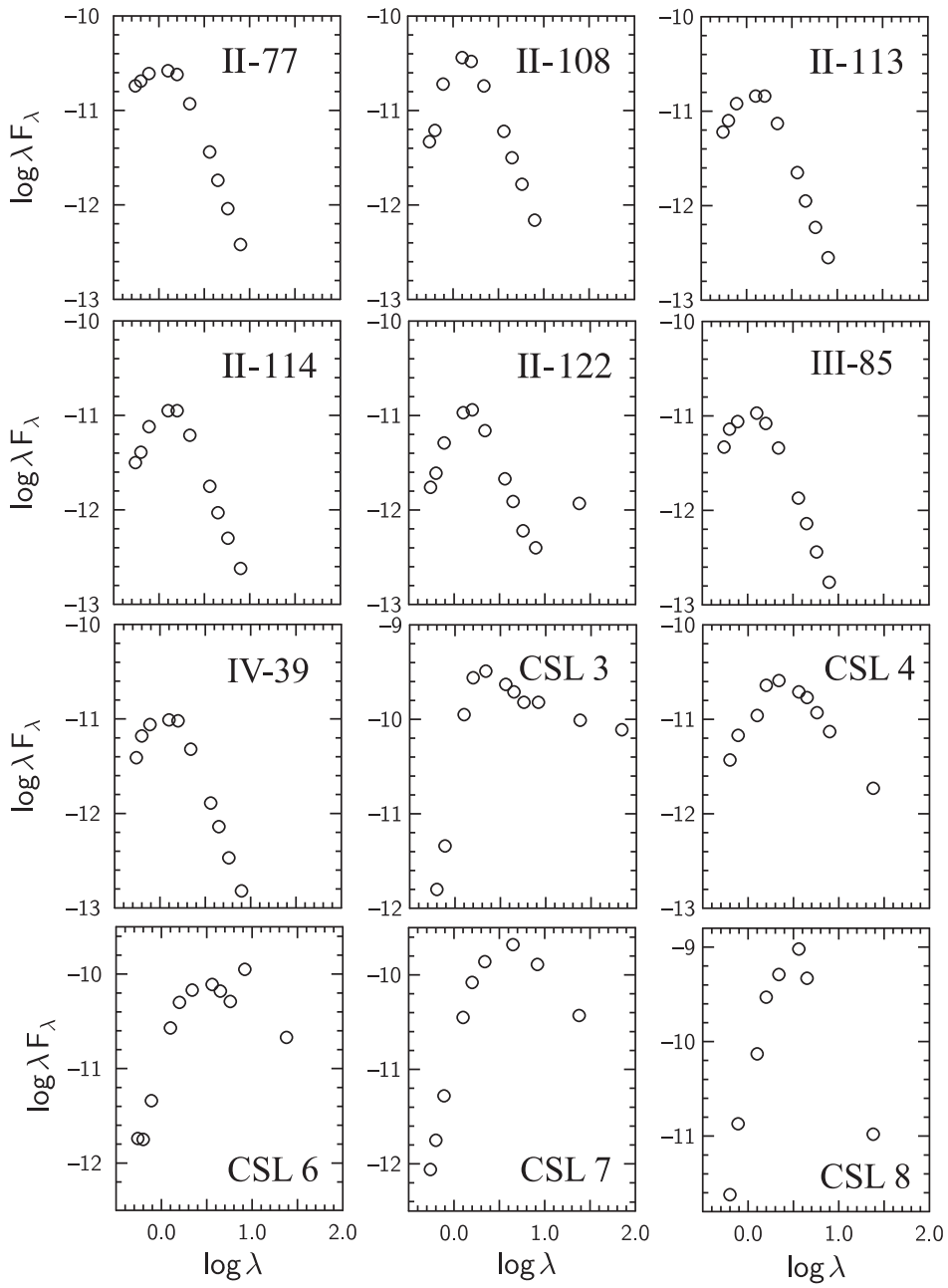


Fig. 4. Spectral energy distributions between $0.5 \mu\text{m}$ and $70 \mu\text{m}$.

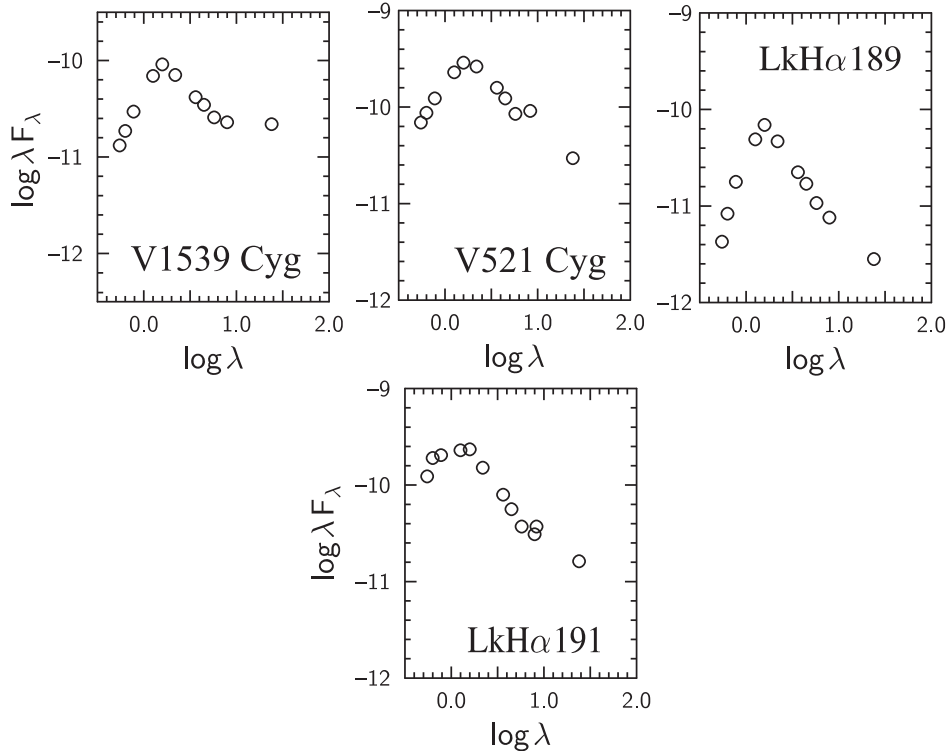


Fig. 4. Continued.

with the Pelican exposure should give 0.005 ct/s which is about the same as the limiting count rate in Pelican. Thus, the non-detection of the Pelican PMS stars in X-rays can be explained by too short HRI exposures.

At the same time, X-ray fluxes of PMS stars are easily detectable in the nearby star-forming regions (Tau/Aur, Oph, Lup, Cha) where the X-ray flux is about 10 times stronger due to their small distances.

6. DISCUSSION OF INDIVIDUAL OBJECTS

In this section we give more information about the investigated objects and discuss the results of spectral classification and emission line intensities. To understand better photometric properties of the stars described, in Figures 5 and 6 we show the $J-H$ vs. $H-K_s$ diagrams for the two groups of the investigated stars.

II-64 = 2MASS J20570757+4341597

This star, as well as other stars with the numbers starting with II and III, are located in the Gulf of Mexico of the dark cloud LDN 935 (TGU 497). Based on the interstellar reddening-free Q_{XZS} vs. Q_{XYV} and Q_{XZS} vs. Q_{YZV} diagrams of the *Vilnius* photometric system the star was suspected to be in the PMS stage of evolution (Laugalys et al. 2006). In both diagrams the star deviates considerably from the main sequence, and such its position can be explained by the presence of emission in the $H\alpha$ line which makes the star brighter in the S passband centered

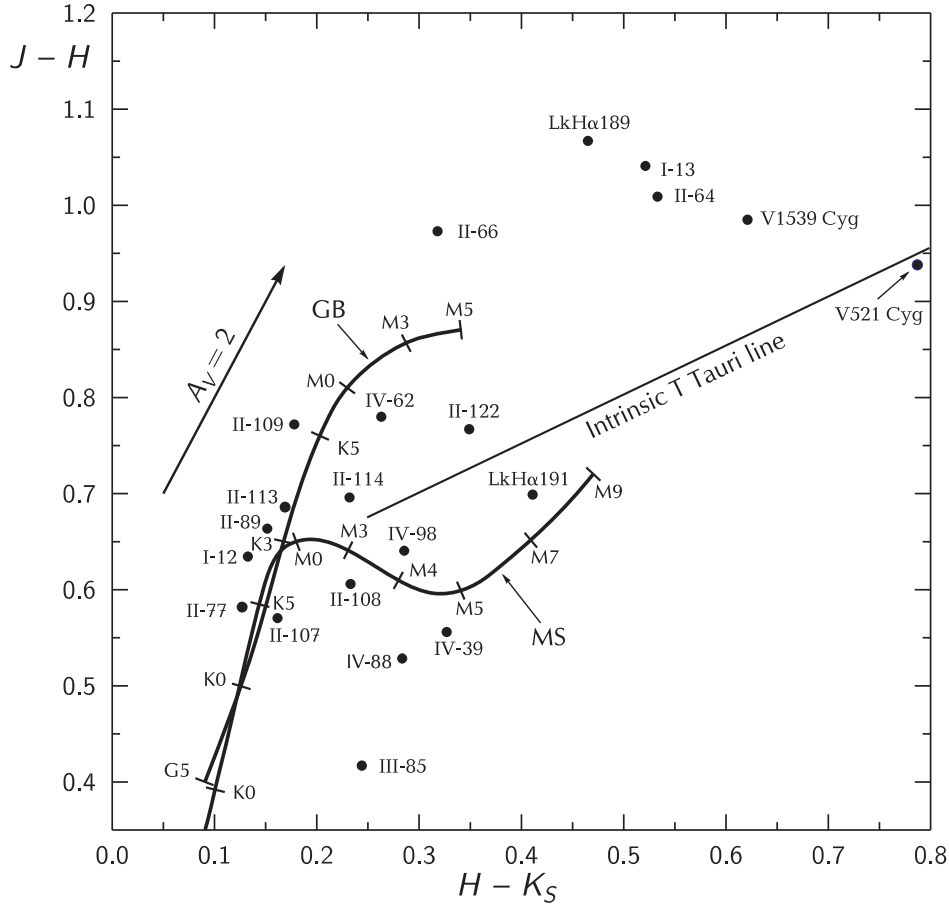


Fig. 5. $J-H$ vs. $H-K_s$ diagram for the stars with $H\alpha$ emission found in their spectra. A few non-emission stars discussed in the text are also plotted. The main-sequence (MS), the giant branch (GB) and the T Tauri star intrinsic lines are shown. The arrow indicates the interstellar reddening vector for $A_V = 2$ mag.

on this line. In the $J-H$ vs. $H-K_s$ diagram (Figure 5) the star lies 0.2 mag above the intrinsic line of T Tauri stars (Meyer et al. 1997). Our spectrum shows that the star is of spectral class K2 with the moderate emission in $H\alpha$ ($EW = -6.8 \text{ \AA}$). Since the star has no measurements in the MSX and *Spitzer* bands, we have no possibility to verify the presence of infrared emission at $\lambda > 3 \mu\text{m}$.

The star is only $6''$ from a slightly brighter star, II-66 = 2MASS J20570786+4341554, classified from *Vilnius* photometry as a K5 dwarf. Its 2MASS colors $J-H = 0.973$ and $H-K_s = 0.318$ place II-66 ~ 0.25 mag above the intrinsic T Tau line. Consequently, the star can be an YSO, too. This is also confirmed by *Spitzer* photometry (Table 4 of Guieu et al. 2009).

II-77 = 2MASS J20572224+4357534

In the *Vilnius* interstellar reddening-free diagrams the star considerably deviates from the main sequence, not less than II-64. In its spectrum, however, $H\alpha$

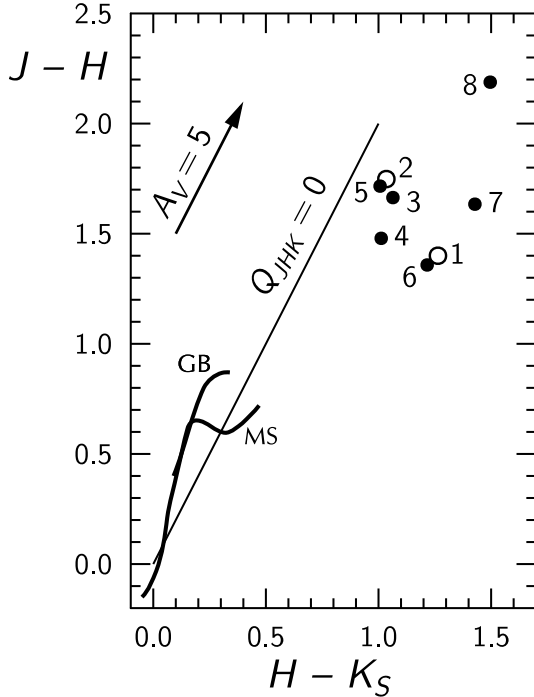


Fig. 6. $J-H$ vs. $H-K_s$ diagram for the investigated stars with $H-K_s > 1.0$. The numbers at the points refer to the CSL numbers in Table 3. The stars with $H\alpha$ emission are plotted as dots, the two non-emission stars as circles. The intrinsic lines of the main sequence and giants, the interstellar reddening vector for $A_V = 5$ mag and the reddening line separating stars with positive and negative Q_{JHK} values are also shown.

emission is much fainter and the spectral class is earlier (G8). In the $J-H$ vs. $H-K_s$ diagram (Figure 5) the star lies close to the K dwarf sequence. The star was measured in the four *Spitzer* IRAC bands, and its energy distribution (Figure 4) does not show any infrared emission. Consequently, the star seems to be a slightly reddened G dwarf with chromospheric activity. However, in this case it is difficult to explain its anomalous position in the diagrams of the *Vilnius* system. If the star is G8 V, its distance is 580 pc, i.e., close to the distance of the NAP complex.

II-108 = 2MASS J20574880+4350236

In the Q, Q diagrams of the *Vilnius* system the star deviates from the K-dwarf sequence as much as the stars II-64 and II-77. However, our spectrum shows that the star differs from the two previous stars being of spectral class M3.5e and having fainter $H\alpha$ emission ($EW = -0.2 \text{ \AA}$). In the $J-H$ vs. $H-K_s$ diagram (Figure 5) the star lies close to the intrinsic position of M3 V stars with no infrared excess. Its energy distribution (Figure 4), constructed from the 2MASS and *Spitzer* observations, also evidences a normal star without envelope. Most probably the star is a M-dwarf with weak chromospheric activity. Its $V = 16.59$ and $M_V = +10.9$ (for a M3.5 V star) correspond to a distance from the Sun of 137 pc, i.e., the star cannot have any relation to the NAP complex.

II-109 = 2MASS J20575005+4350569

Interstellar reddening-free parameters in the *Vilnius* system classify the star as a dwarf of spectral class M1, but the classification is of low accuracy since the star is quite faint ($V = 17.88$) and its ultraviolet magnitudes U and P have not been measured. The S magnitude on $H\alpha$ shows a mild indication of emission. 2MASS

color indices of this star, $J-H = 0.772$ and $H-K_s = 0.178$, place it well above the intrinsic T Tauri star line (Figure 5). However, the magnitudes J , H and K_s are of low accuracy, with the 0.05–0.07 mag errors. The star is absent both in the MSX and in *Spitzer* lists, so we cannot verify if the envelope is present. In our spectrum it looks like a G-type star with $H\alpha$ filled with emission but this does not help to understand the behavior of its photometric indices.

II-113 = 2MASS J20575651+4352362

In the *Vilnius* system the star is classified as K dwarf with possible $H\alpha$ emission. In the Q, Q diagrams, indicating the emission, the star lies close to II-109. Both stars are also similar in our spectra, they are classified as Ge stars with $H\alpha$ filled with emission. In the $J-H$ vs. $H-K_s$ diagram (Figure 5) the star lies close to the intrinsic position of M0 V star, but it can be a reddened G-type star, too. IRAC magnitudes measured by *Spitzer* show no infrared excess (Figure 4). Thus, both stars (II-109 and II-113) could be reddened G main sequence stars but this does not explain their considerable excesses of radiation in the *Vilnius S* passband. These stars may have been in a particularly active phase when observed with *Vilnius* photometry, and quiet when observed spectroscopically.

II-114 = 2MASS J20575750+4350089

In the *Vilnius* system the star is classified as M2e. In the $J-H$ vs. $H-K_s$ diagram (Figure 5) it lies in the upper part of the early M dwarf band, so there are no indications of the presence of the envelope. This is confirmed by the *Spitzer* fluxes (Figure 4). Our spectrum shows that the star is of spectral class M1 with small emission in $H\alpha$ ($EW = -1.8 \text{ \AA}$). The star can be either an unreddened field dwarf with chromospheric activity, located at 350 pc, or a post-T Tauri star at the front edge of the NAP complex.

II-117 = V 1539 Cyg = 2MASS J20575986+4353260

This star is a known emission-line star (LkH α 185), T Tauri type variable. The *Vilnius* reddening-free parameter Q_{XZS} shows very strong anomaly caused by strong emission in $H\alpha$, which from our spectrum gives $EW = -79.4 \text{ \AA}$. Ca II and O I lines are also in emission. In the $J-H$ vs. $H-K_s$ diagram (Figure 5) the star lies by 0.12 mag above the intrinsic T Tauri line. The *Spitzer* fluxes exhibit the presence of a considerable thermal emission from the dust envelope (YSO of class II, Figure 4). Our spectrum shows its spectral class G5e.

II-122 = 2MASS J20580604+4349328

In the *Vilnius* system the star is classified as a K–M dwarf with possible emission, but due to its faintness ($V = 17.66$) the ultraviolet magnitudes U and P were not measured, the violet X and the blue Y magnitudes are also of low accuracy. In the $J-H$ vs. $H-K_s$ diagram (Figure 5) the star lies 0.05 mag above the intrinsic T Tauri line. The *Spitzer* fluxes exhibit the presence of emission in I_4 and $M1$ bands (at $\lambda \geq 8 \mu\text{m}$) confirming the YSO status of the star. Our spectrum gives the spectral class K7e with strong $H\alpha$ line ($EW = -41.1 \text{ \AA}$). If the star is close to the main sequence, its distance is similar to the NAP complex.

III-85 = 2MASS J20593535+4352035

This object was found peculiar by Laugalys et al. (2006) due to an excess of radiation in the passband S . In the $J-H$ vs. $H-K_s$ diagram (Figure 5) the star appears to be of early type with a considerable reddening. Our spectral classification gives the spectral class A0 with the emission component inside the

H α line, shifted longward from the absorption, or the strong absorption shifted shortward of emission (the P Cygni profile). The SED curve in the infrared does not show any excess (Figure 4). The star III-85 is far behind the NAP complex, see the description of the following star.

IV-5 = 2MASS J20535187+4424100

This and the following three stars are located in Area IV (Laugalys et al. 2006), above Pelican's beak, near the two bright stars, HD 199081 (57 Cyg) and HD 199178. The star IV-5 could not be classified in the *Vilnius* system – its color indices are very peculiar. A considerably diminished Q_{XZS} parameter was in favor of the presence of H α emission. 2MASS magnitudes are given with a very low accuracy and are useless. No doubt, its image was affected by a nearby extremely red AGB star 2MASS J20535282+4424015 = StRS 383 discussed by Neckel et al. (1980) and Eiroa et al. (1983) and included into a list of highly reddened stars by Stephenson (1992). The brightness of the latter star drastically increases with increasing wavelength: its blue magnitude is about 20, $V = 16.7$, $N(840\text{ nm}) = 10.4$, $J = 6.2$, $H = 4.3$, $K = 3.2$ and $L = 2.0$. Thus, in the 2MASS survey the star IV-5 is immersed in the oversaturated image of StRS 383. We classified the spectrum of IV-5 as A0e, it is quite similar to that of the star III-85 with strong H α absorption line having a redshifted emission component. Both these stars should be farther than 2.7 kpc.

IV-39 = 2MASS J20542554+4423019

In the *Vilnius* system the star is classified as a K or M dwarf with emission. In the $J-H$ vs. $H-K_s$ diagram (Figure 5) the star lies on the sequence of M-dwarfs. Our spectral classification gives the spectral class M3 with a faint emission in H α ($EW = -1.2\text{ \AA}$). The SED curve in the infrared does not show any excess (Figure 4). Consequently, the star seems to be a chromospherically active M dwarf. For $V = 17.37$, $M_V = +10.4$ and no reddening we obtain a distance of 250 pc, i.e., it is much closer than the NAP complex.

IV-62 = 2MASS J20544534+4433027

In the *Vilnius* system the star is classified as a reddened K0 dwarf with emission. In the $J-H$ vs. $H-K_s$ diagram (Figure 5) the star lies 0.1 mag above the intrinsic T Tauri line. Our spectral classification gives the spectral class K0 with faint emission in H α ($EW = -1.8\text{ \AA}$). With $V = 17.24$, $M_V = +5.9$ and $A_V = 3.21$ (Laugalys et al. 2006) its distance is 420 pc, i.e. close to the distance of the NAP complex. Thus, the star can be either a chromospherically active field dwarf or a post T Tauri star immersed in the dark cloud.

IV-98 = 2MASS J20551122+4424052 In the *Vilnius* system the star is classified as B star with emission. In the $J-H$ vs. $H-K_s$ diagram (Figure 5) the star lies close to the M4V position where the star could appear due to large interstellar reddening. Our spectrum around H α shows that it could be a mid-B star, if H α is partly filled-in by emission. Probably the star is a mild Be star with $A_V \approx 6.7$. If we accept it is a B5 star on the main sequence, its distance is about 1.2 kpc.

CSL 3 = 2MASS J20485070+4349496

The star is located in the direction of the Pelican nebula. Its colors $J-H = 1.66$, $H-K_s = 1.06$ place the star ~ 0.5 mag above the intrinsic T Tauri line, with $Q_{JHK_s} = -0.46$ (Figure 6). The IRAS 20472+4338 source with the coordinates corresponding to an angular distance of $101''$ from CSL 3 probably is not related

to this star. Our spectrum shows strong emission lines of $H\alpha$ ($EW = -30.5 \text{ \AA}$) and Ca II, the spectral class is G0e. Spectral energy distribution (Figure 4) is typical of YSO of Class II (T Tauri star). If the star is located in the NAP complex (500 pc) and has $A_K \approx 2$ mag, its absolute magnitude M_K should be close to -2 mag.

CSL 4 = 2MASS J20493219+4417031

The star is located also in the direction of Pelican. The colors $J-H = 1.48$ and $H-K_s = 1.01$ place the star ~ 0.4 mag above the intrinsic T Tauri line, with $Q_{JHK_s} = -0.54$ (Figure 6). Our spectrum shows extremely strong emission in $H\alpha$ ($EW = -151.3 \text{ \AA}$) and strong emissions in Ca II, the spectral class is F0e. The spectral energy distribution (Figure 4) shows an increase of intensity in the mid-infrared up to the *Spitzer* MIPS passband at $24 \mu\text{m}$, but this increase is not so striking as in CSL 3. This seems to be in contradiction with its strong emission lines in the far red spectrum. Based on *Spitzer* photometry the star was also included in the list of potential YSOs (Guieu et al. 2009). At a distance of 500 pc and $A_K \approx 2$ mag, its absolute magnitude M_K should be close to $+0.9$ mag.

CSL 5 = 2MASS J20533846+4428484

The star is located in the direction of Pelican, close to the star IV-5 described above. The colors $J-H = 1.72$ and $H-K_s = 1.01$ place the star ~ 0.6 mag above the intrinsic T Tauri line, its $Q_{JHK_s} = -0.30$ (Figure 6). However, this position is the result of considerable moving along the reddening line starting from A-type stars. Our classification gives the spectral class A5 with the emission component inside the $H\alpha$ line, longward from the absorption (the P Cygni like profile). In this respect the star is quite similar to III-85 and IV-5 described above. Since the star was observed neither by MSX nor *Spitzer*, we have no possibility to construct its spectral energy distribution in the mid-infrared. The star can be in a post Herbig Ae evolutionary stage with a remnant disk or envelope. At a distance of the NAP complex and $A_K \approx 1.9$ mag, its absolute magnitude M_K should be $+0.3$ mag.

CSL 6 = 2MASS J20544690+4448197

The star is located at the upper right edge of the North America nebula. Its $J-H = 1.36$ and $H-K_s = 1.22$ place the star close to the intrinsic T Tauri line, with $Q_{JHK_s} = -1.07$ (Figure 6). Our spectrum shows that this is a heavily reddened Ae star with strong emission lines of $H\alpha$ ($EW = -82.9 \text{ \AA}$) and Ca II. The spectral energy distribution (Figure 4) shows an enhanced intensity in the IRAC and MIPS bands which is typical of YSO of Class III. The MSX $8.3 \mu\text{m}$ band measurement gives much brighter value ($\log \lambda F_\lambda = -9.95$) than the interpolated *Spitzer* data. Maybe, this is related with the IR emission variability. We conclude that CSL 6 is a typical medium-mass Herbig Ae-type YSO. The star is recognized as an emission star in the IPHAS survey. At a distance of the NAP complex and $A_K \approx 2.4$ mag, its M_K is close to -0.6 mag.

CSL 7 = 2MASS J20562782+4525234

The star is located in the direction of the upper part of the North America nebula. Its $J-H = 1.63$ and $H-K_s = 1.43$ place the star above the intrinsic T Tauri line, with $Q_{JHK_s} = -1.22$ (Figure 6). However, the star has no relation to T Tauri stars, being a heavily reddened Herbig Ae star of medium-mass. Our spectrum shows the strongest emission of $H\alpha$ among all of the investigated stars ($EW = -168.7 \text{ \AA}$). Emission lines of O I, Ca II and P 9 are also strong, spectral class is close to A0. The spectral energy distribution (Figure 4) shows very strong interstellar (and circumstellar) reddening and the presence of enhanced intensity

in the IRAC and MIPS bands, typical of YSOs of Class III. At a distance of the NAP complex and $A_K \approx 2.8$ mag, its M_K is close to -1.8 mag.

CSL 8 = 2MASS J21010487+4342340

The star is located in the direction of a bright nebula to the left from the Gulf of Mexico. Its $J-H = 2.19$ and $H-K_s = 1.50$ place the star about 0.75 mag above the intrinsic T Tauri line, with $Q_{JHK_s} = -0.80$ (Figure 6). Our spectral classification shows that it is a K3 supergiant with moderate emission in $H\alpha$ ($EW = -5.0$ Å). Its spectral energy distribution (Figure 4) shows a very large interstellar reddening, with maximum in the $3.6 \mu\text{m}$ IRAC band. Very strong interstellar reddening is essential to explain its position in the $J-H$ vs. $H-K_s$ diagram. If the star is K3 Iab, its $M_K \approx -9.8$ mag. With $K_s = 8.11$ and $A_{K_s} = 2.7$ mag we get a distance of 11 kpc, i.e., the star can be located in the Outer spiral arm. The $H\alpha$ emission seen in the spectrum can originate in a nebula at the close vicinity of the supergiant.

Stars without emission lines

In the spectra of some stars, which in the paper Laugalys et al. (2006) were suspected to have $H\alpha$ in emission, emission was not found. These stars are listed in Table 3, where the fifth column gives spectral classes estimated from our spectra. Most of these stars were found to be M-dwarfs, not K-dwarfs as they were classified in the *Vilnius* system. This may mean that K and M dwarfs are not sufficiently represented among the standard stars used to classify stars from the photometric data. On the other hand, most of these stars are fainter than $V = 16$ mag, and for many of them ultraviolet magnitudes U and P were too faint to be measured with good accuracy.

It should be noted that the classification of some of these stars contradicts their positions in the $J-H$ vs. $H-K_s$ diagram. For example, the star I-13 lies about 0.2 mag above the intrinsic T Tauri line. If the star is a M2 dwarf, it should be considerably shifted along the interstellar reddening line ($A_V \approx 4$ mag). However, the spectrum of I-13 does not show such reddening. The stars I-12, II-89 and II-107 have too blue $H-K_s$ colors for the spectral class dM2. The star IV-88, if it were G dwarf, should have considerable reddening in agreement with its spectrum shape (unfortunately, quite noisy). The infrared colors of CSL 1 and CSL 2 also do not agree with the finding that these stars are K0 and G8 dwarfs: none of normal G-K stars can have such negative values of Q_{JHK} (Figure 6). In some cases these discrepancies can be explained by unresolved duplicity of the stars. For example, the image of the star I-12 in DSS2 is clearly asymmetric, this suggests the star to be a binary. The stars CSL 1 and CSL 2 can be physical binaries with L-dwarf components which might be responsible for their strong infrared excesses.

Assuming that eleven K and M stars in Table 3 are of luminosity V, we get their interstellar extinctions and distances given in the last two columns. It is evident that all these stars are located in front of the LDN 935 cloud. The luminosity class of the III-71 star of Table 3 is not known but it is evident that it is a distant object located far behind the NAP complex.

7. CONCLUSIONS

The present spectral investigation shows that the suspected $H\alpha$ emission stars in the NAP complex do not constitute a homogeneous group. Fourteen of them were found to be normal G-, K- and M-dwarfs without emission. This may indicate that their emission in $H\alpha$ is variable and sometimes disappears. An alternative

Table 3. Stars for which our spectra do not show the presence of strong emission lines.

Name	RA (2000)	DEC (2000)	V	Sp	A_V	d (pc)
I-12*	20:54:40.64	+43:52:47.2	17.2	dM2.5	0.62	184
I-13*	20:54:42.08	+43:45:57.3	17.5	dM2	0.46	268
I-53	20:55:27.48	+43:53:17.8	17.5	dM1	1.08	260
I-61	20:55:33.59	+43:52:19.8	16.8	dM1	0.62	233
I-62	20:55:34.93	+43:49:44.2	16.0	dM3.5	0.21	97
II-50	20:56:51.69	+43:42:52.0	15.3	dK3	0.71	400
II-67	20:57:09.06	+43:44:44.5	17.3	dM3	0.00	240
II-89*	20:57:28.64	+43:58:31.6	16.3	dM2	0.46	156
II-102	20:57:43.26	+43:56:31.9	16.6	dM4	0.00	108
II-107*	20:57:48.00	+43:42:54.6	17.4	dM2	0.50	256
II-118	20:57:59.93	+43:51:21.2	16.8	dM2	0.62	178
III-71	20:59:29.29	+43:45:56.5	16.8	A0		
IV-88**	20:55:05.18	+44:36:31.1	17.9	G8:		
CSL 1*	20:46:46.94	+43:17:34.6	17.5	dK0		
CSL 2*	20:48:30.50	+44:22:54.6	17.0(r)	dG8		

Notes. * These stars are discussed in the text; ** IV-88, noisy spectrum.

possibility is related to the errors of photometric classification due to insufficient accuracy of CCD photometry or calibration of photometric parameters of red dwarfs (or both). In some cases, the peculiarity of photometric color indices can be the result of unresolved binarity. Two stars without emission, CSL 1 and CSL 2, are very strong in the near infrared; their infrared excesses are far too large to be of interstellar origin. These stars can be binaries with the cool components of late M or L spectral types. The infrared excess of I-13 may be of the same origin.

The remaining 19 stars in our list exhibit different strengths of $H\alpha$ emission and different spectral types. Among these stars seven show strong emission, six show medium and weak emission, and in six spectra the $H\alpha$ line is filled by emission or has an emission component. In spectral classes we have the following distribution: one is a mid-B star, five A stars, one F star, five G stars, four K stars and three M stars. For six stars the mid-infrared thermal emission in the dust envelope was found; seven stars do not show the presence of such emission and for six stars the data were missing.

Only eight stars in the investigated emission-line star sample seem to be members of the NAP complex. Five of them belong to the group of eight suspected YSOs with negative values of Q_{JHK_s} and $H-K_s > 1.0$. This means that a considerable fraction of true YSOs, related to the NAP complex, is expected among stars with negative Q_{JHK_s} values. Tens of such objects in our list selected from 2MASS are fainter than magnitude 17 and they were not accessible to the telescope used. Many more YSOs should be present among the objects with $H-K_s$ between 0.5 and 1.0. Consequently, the prediction of a large PMS population in the NAP complex still holds to be true. A big list of possible YSOs in the region, suspected with the help of *Spitzer* photometry (Guieu et al. 2009), is a confirmation.

The most effective methods for their detection are deep surveys of $H\alpha$ emission stars using photometry in the *Vilnius* or IPHAS systems. To confirm the

evolutionary status of the suspected young objects we need their red spectra for measuring H α intensity and also for checking the presence of the Li I doublet at 6708 Å which is a nice test of the star youth. Although in our spectra of some stars the Li line is visible, for its exact identification and *EW* estimation a better *S/N* ratio is desirable. Mid-infrared photometry in $\lambda > 5 \mu\text{m}$ is essential to verify the presence of circumstellar envelopes, and X-ray observations can confirm the presence of active coronae, a characteristic feature among T Tauri and post-T Tauri stars.

ACKNOWLEDGMENTS. We are thankful to the Steward Observatory for the observing time, to Luisa Rebull for the *Spitzer* data and to Edmundas Meištas and Stanislava Bartasiūtė for their help in preparing the paper. The use of the 2MASS, MSX, IPHAS, SkyView, Gator and Simbad databases and the IRAF program package is acknowledged.

REFERENCES

- Comerón F., Pasquali A. 2005, *A&A*, 430, 541
 Corbally C. J., Straižys V. 2008, *Baltic Astronomy*, 17, 21
 Corbally C. J., Straižys V. 2009, *Baltic Astronomy*, 18, 1
 Danks A. C., Dennefeld M. 1994, *PASP*, 106, 382
 Drew J. E., Greimel R., Irwin M. J. et al. 2005, *MNRAS*, 362, 753
 Eiroa C., Hefele H., Zhong-yu Q. 1983, *A&AS*, 54, 309
 Egan M. P., Price S. D., Kraemer K. E. et al. 2003, *The Midcourse Space Experiment Point Source Catalog*, version 2.3, AFRL-VS-TR-2003-1589; available at CDS: MSX6C Infrared Point Source Catalog, V/144
 Gagné M., Caillaut J.-P., Stauffer J. R. 1995, *ApJ*, 445, 280
 Giesekeing F. 1973, *Veröff. Astron. Inst. Bonn*, Nr. 87
 Giesekeing P., Schumann J. D. 1976, *A&AS*, 26, 367
 González-Solares E. A., Walton N. A., Greimel R., Drew J. E. 2008, *MNRAS*, 388, 89
 Guieu S., Rebull L. M., Stauffer J. R. et al. 2009, *ApJ*, 697, 767
 Herbig G. H. 1958, *ApJ*, 128, 259
 Kohoutek L., Wehmeyer R. 1997, *H-alpha Stars in Northern Milky Way*, *Abh. Hamburger Sternw.*, 11, Teil 1+2 = CDS catalog III/205
 Lasker B. M., Lattanzi M. G., McLean B. J. et al. 2008, *AJ*, 136, 735; *Simbad Catalog I/305*, version GSC 2.3.2
 Laugalys V., Straižys V., Vrba F. J., Boyle R. P., Philip A. G. D., Kazlauskas A. 2006, *Baltic Astronomy*, 15, 483
 Marcy G. W. 1980, *AJ*, 85, 230
 Meyer M. R., Calvert N., Hillenbrand L. A. 1997, *AJ*, 114, 288
 Neckel Th., Harris A. W., Eiroa C. 1980, *A&A*, 92, L9
 ROSAT Team 2000a, *ROSAT News*, No.71; available at CDS: The ROSAT Source Catalog of Pointed Observations with the High Resolution Imager (HRI, 1RXH), IX/28A
 ROSAT Team 2000b, *ROSAT News*, No.72; available at CDS: The ROSAT Source Catalog of Pointed Observations with the Position Sensitive Proportional Counter (PSPC, 2RXH), IX/30
 Stephenson C. B. 1992, *AJ*, 103, 263

- Straižys V., Corbally C. J., Laugalys V. 2008, *Baltic Astronomy*, 17, 125
- Straižys V., Eimontas A., Sūdžius et al. 1998, *Baltic Astronomy*, 7, 589
- Straižys V., Laugalys V. 2007, *Baltic Astronomy*, 16, 327
- Straižys V., Laugalys V. 2008, *Baltic Astronomy*, 17, 143
- Tsvetkov M. K. 1975, *Astrofizika*, 11, 579
- Voges W., Aschenbach B., Boller Th. et al. 1999, *A&A*, 349, 389; available at
CDS: ROSAT All-Sky Survey Bright Source Catalog (1RXS), IX/10
- Voges W., Aschenbach B., Boller Th. et al. 2000, *IAUC*, 7432; available at CDS:
ROSAT All-Sky Survey Faint Source Catalog, IX/29
- Welin G. 1973, *A&AS*, 9, 183
- Witham A. R., Knigge C., Drew J. E. et al. 2008, *MNRAS*, 384, 1277